Study on microstructure and properties of Mg-alloy surface alloying layer fabricated by EPC

***Chen Dongfeng, Dong Xuanpu, Fan Zitian, Xu Qian and Zhang Xiong**

(State Key Laboratory of Material Processing and Die & Mold Technology, Huazhong University of Science and Technology,Wuhan 430074, China)

Abstract: AZ91D surface alloying was investigated through evaporative pattern casting (EPC) technology. Aluminum powder (0.074 to 0.104 mm) was used as the alloying element in the experiment. An alloying coating with excellent properties was fabricated, which mainly consisted of adhesive, co-solvent, suspending agent and other ingredients according to desired proportion. Mg-alloy melt was poured under certain temperature and the degree of negative pressure. The microstructure of the surface layer was examined by means of scanning electron microscopy. It has been found that a large volume fraction of network new phases were formed on the Mg-alloy surface, the thickness of the alloying surface layer increased with the alloying coating increasing from 0.3 mm to 0.5 mm, and the microstructure became compact. Energy dispersive X-ray (EDX) analysis was used to determine the chemical composition of the new phases. It showed that the new phases mainly consist of β-$Mg_{17}Al_{12}$, in addition to a small quantity of inter-metallic compounds and oxides. A micro-hardness test and a corrosion experiment to simulate the effect of sea water were performed. The result indicated that the highest micro-hardness of the surface reaches three times that of the matrix. The corrosion rate of alloying samples declines to about a fifth of that of the as-cast AZ91D specimen.

Key words: EPC; magnesium alloy; surface alloying; corrosion rate
CLC number: TG249.5/174.445 Document code: A Article ID: 1672-6421(2010)01-013-06

Nowadays, with the 21th century's wish for sustainable development of green metallic construction materials, more and more attention is paid to magnesium-based alloys in the materials research field. This is because it has the advantages of low density, high specific strength and specific rigidity, and good castability and workability [1-2]. With the development of society, Mg-alloys have been extensively applied in many fields such as the automotive, aerospace and electronic industries. The research and application of Mg-alloys are not perfect compared with aluminum alloys at present. A major stumbling block that restricts the development and commercial applications of magnesium alloys is their poor corrosion resistance, which can't meet the requirement under complicated environment [3]. In order to improve corrosion resistance and friction resistance of Mg-alloys, a number of surface treatment technologies have been developed [4-5], such as chemical conversion treatment [6-7], surface anode oxidation [8-9], vapour deposition [10-11], phosphating [12], and laser treatment [13].

***Chen Dongfeng**

Male,born in December,1980, Ph.D. Direction of research: Surface alloying and composite materials.
E-mail:cdf626@163.com
Received: 2009-03-19; Accepted: 2009-05-20

The previous studies mainly concentrated on the solid phase diffusion, however, the diffusion layer is too thin to protect the substrate effectively. Mg-alloy surface alloying through casting technology can make use of some advantages of casting, for instance, the good penetrability of molten metal, and the melt permeating the alloying coating after pouring the melt. The powder particles melt and diffuse within the interface between the substrate and particles. At the interfaces between the alloying coating and the melt, the occurrence of metallurgical fusion gives birth to the formation of an alloying layer on the matrix, whose thickness can reach hundreds of microns. The present surface alloying investigation mostly focuses on cast iron, cast steel and other high melting point metals. For magnesium alloys there is little research in this aspect, and related literatures and reports are not much so far.

In this paper, a surface alloying layer was fabricated on the Mg alloy substrate through EPC based on the previous surface alloying investigation [14-18]. The aluminum powder was taken as the alloying element, alloying coating was spread on the surface of the EPS pattern. The powder began melting when it obtained enough energy from the molten liquid matrix and formed alloying layer through the reaction between the two. The microstructure and micro-hardness of the surface layer were observed, and the corrosion properties of samples were examined.

1 Experimental procedures

1.1 Matrix and alloying element selection

AZ91D cast magnesium alloy was used as a substrate that applies in the automotive, aerospace and electronics industries ect. The aluminum powder with the size range from 0.104 to 0.074 mm was chosen as the alloying element. The alloying coating was made according to desired ingredients. Table1 shows the chemical composition of the matrix.

Table 1: Chemical composition of tested AZ91D（wt %）

Al	Zn	Mn	Si	Fe	Mg
9.21	0.63	0.29	0.05	0.0038	bal.

1.2 Experimental methods

The EPS foam mould was prepared with a size of 50 mm × 50 mm × 50 mm. Fabrication of the alloying coating is the key technology. The coating is mainly composed of the alloying element (aluminum powder), adhesive, complex additive, organic solvent and other components (suspending agent, surfactant, de-foamer) according to the desired proportions in the experiment. The optimal proportions were attained through test. The surface of the EPS mould was heated firstly to dry, and was coated with the coating, then followed by dry again at 50 ℃.

The surface alloying layer was prepared by EPC technology. The magnesium alloy was poured under the conditions of a temperature of 780 ℃ and a negative pressure of 0.02 MPa. The EPS foam mould was decomposed and vaporized when it met the high temperature liquid substrate, the liquid metal infiltrated into the capillary of the alloying coating under the effect of negative pressure and penetrability. The coating melted gradually because of the heat from the matrix and interacted with the substrate and formed the metallurgical layer. Sketch of the surface alloying set up is shown in Fig. 1.

The specimens were cut along the direction from surface to substrate, ground with 600#, 800#, and 1500# emery paper, then polished using standard metallographic techniques, degreased with ethanol and acetone, and finally etched with 4% nitric acid in ethanol solution. Samples were observed to analyze microstructure using SEM. Energy dispersive X-ray (EDX) analysis was used to determine the chemical composition of new phases. Tests were carried out on the micro-hardness and the distribution of aluminum content.

The corrosion test system basically consists of CorrTest software, data collection card and CT-B constant voltage apparatus. Electrochemical polarization tests were performed to observe the corrosion behavior of the surface alloying layer. A comparison of polarization curves was made between surface alloying samples and as-cast samples. In this test, a standard three electrode configuration was used: a saturated calomel electrode (SCE) was used as the reference electrode and platinum as the counter electrode, with different samples as the working electrode with a working area of 1 cm^2. The corrosion solution was 3.5wt%-NaCl to simulate sea water. Specimens were immersed in the test solution and a polarization scan was conducted from –0.5 V to 0.5 V at a scan rate of 0.2 mV/s.

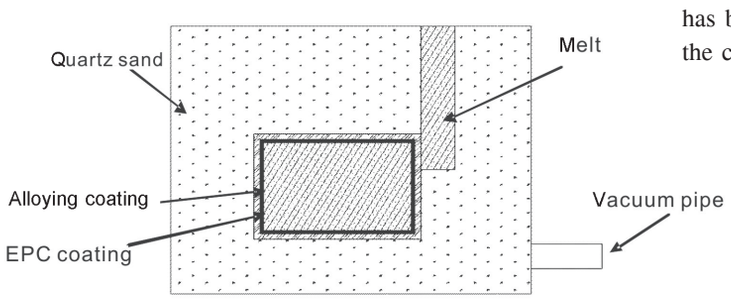

Fig.1: Sketch of the surface alloying setup

2 Results and discussion

2.1 Microstructure analysis

Figure 2 (a) and (b) show the surface microstructures of as-cast and surface alloying samples, respectively. On the basis of previous research, the AZ91 consists of a magnesium rich matrix (α-phase) and an aluminum rich inter-metallic species, $Mg_{17}Al_{12}$(β-phase) that is precipitated along the grain boundaries. Figure 2 (b) shows the alloying surface microstructure. It is obvious that there are a large number of new phases that have a network shape in the surface layer of the sample. The surface layer thickness can be up to 200 μm. The chemical composition of the new phases, determined by energy dispersive X-ray (EDX) is listed in the Table 2. It shows that the aluminum content has an average of about 30wt% (in Fig. 3), which is significantly higher than that of the Mg alloy matrix. There is a small amount of oxygen that maybe come from the water of the coating or some oxides in the liquid metal. It has been proved that the alloying powder melted as a result of energy from the liquid metal and reacted with the substrate during the alloying process forming new phases. Based on the analysis of the Mg-Al binary phase diagram, a conclusion can be drawn that the new phases are mostly $Mg_{17}Al_{12}$, plus some inter-metallics and oxides.

From Fig. 4 the effect of the alloying coating thickness on the microstructure of surface alloying layer can be seen. It has been found that a good alloying layer was formed when the coating thickness was 0.3 mm or 0.5 mm. Moreover, the

Table 2: The chemical composition of new phase

Element	wt%	at%
O	7.38	11.14
Mg	60.26	59.88
Al	32.36	28.98

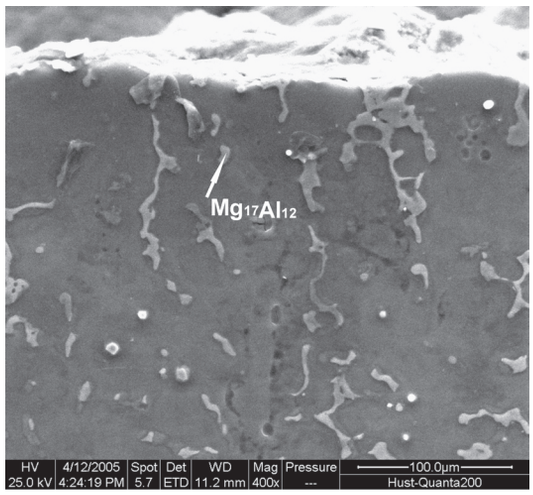

(a) Microstructure of as-cast AZ91D

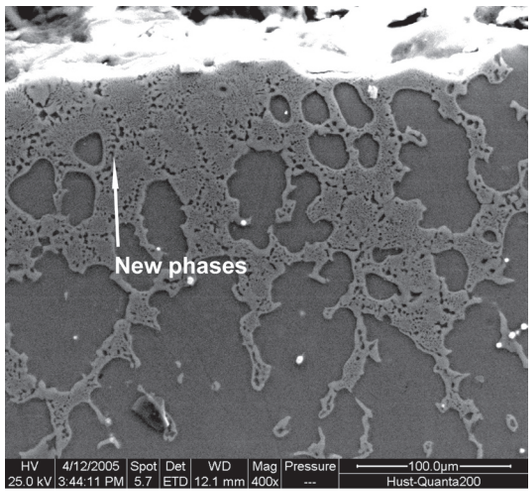

(b) Microstructure of alloying surface layer

Fig.2: SEM microstructure of as-cast and alloying samples

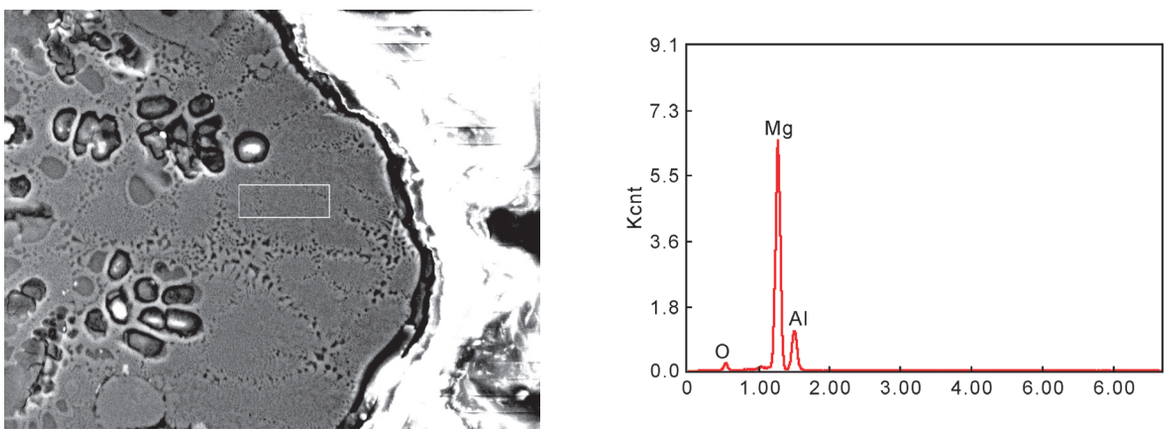

Fig. 3: The result of energy dispersive X-ray analysis in the surface layer

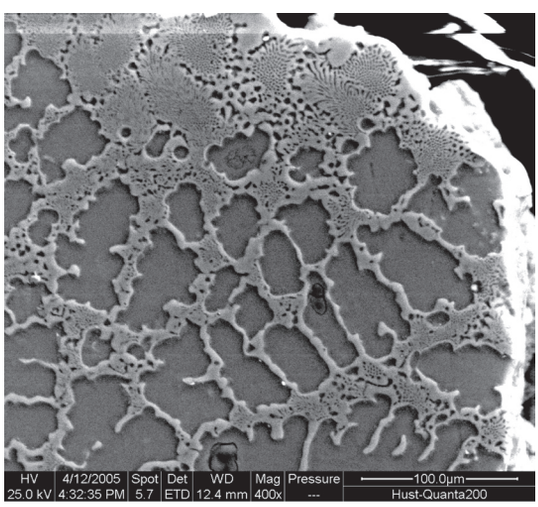

(a) Coating thickness 0.3 mm

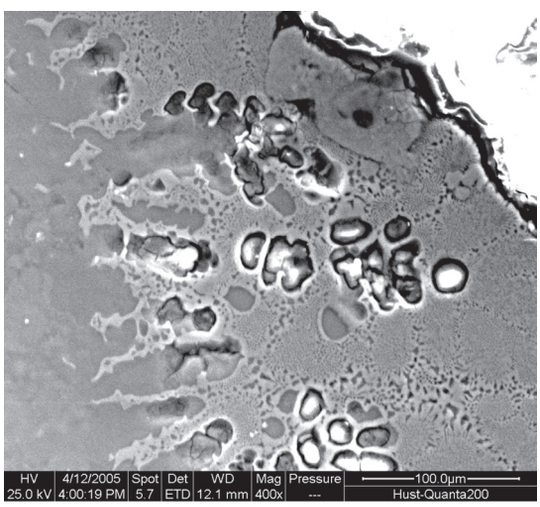

(b) Coating thickness 0.5 mm

Fig. 4: The effect of coating thickness on alloying layer

alloying layer increased gradually with an increase in the coating thickness. The microstructure became compact and evenly distributed, and the whole alloying layer thickness was increased. The new composite layer was formed because the energy from the liquid metal melted the alloying metal powder, which then mixed with the liquid substrate and reacted, forming the new surface layer on the matrix. On one hand, when the alloying coating was thinner, the liquid metal

provided enough energy to both melt the powder entirely and keep the temperature high, allowing the alloying element to diffuse evenly. On the other hand, the thinner coating was easily scattered when poured the liquid metal, so it is difficult to form a dense alloying layer on the matrix surface. With an increasing coating thickness, the alloying element diffusion rate declined when the energy kept constant. Therefore the latter has a good advantage of forming new phase layer on the matrix compared with the former.

2.2 The formation mechanism of the surface alloying layer

The process of surface alloying can be divided into several different stages. Firstly, the EPS foam mould was decomposed when it met the molten liquid matrix. The vapor was removed from the sand mould by the negative pressure. It can be explained from thermodynamics, that the adhesive in the alloying coating burned and decomposed owing to the energy it received from the liquid metal. At the same time, energy from liquid metal transferred to alloying metal powder and melting it. The new phases were formed during the metallurgical fusion. The negative pressure enhanced the fluidity of the liquid metal and its infiltration into the alloying coating in such a short time. A good alloying layer on the surface was formed when the liquid temperature declined. The whole alloying process is illustrated in Fig. 5. Before pouring the powder was firmly bonded by the adhesive. The adhesive burned and changed into gas when the high temperature liquid was poured. This gas was removed through the sand mould as the result of the negative pressure.

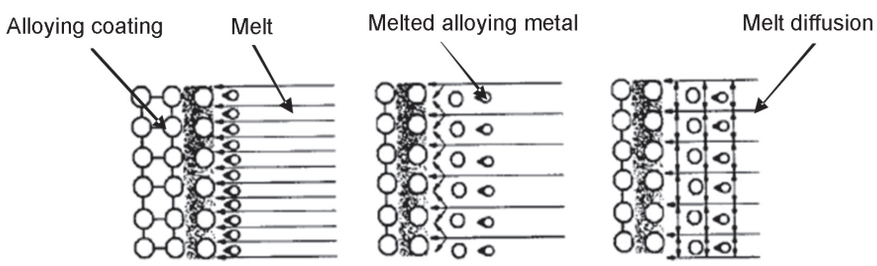

Fig. 5: The sketch of surface alloying layer forming process

2.3 Surface alloying layer properties analysis

2.3.1 Micro-hardness (HV)

Distribution of HV hardness of sample along the direction from the surface into the matrix is shown in Fig. 6. It indicates that the hardness is consistent with the proportion of new phases, the micro-hardness increases gradually with increasing new phases. The hardness firstly increases and then decreases from the surface into the matrix. According to previous microstructure analysis, it is evident that new phases make up a large proportion on the surface. As shown in Fig. 6, the hardness is at it's highest value around HV160, where the distance is 50–100 μm from the surface and it then declines with distance from the surface to substrate, HV55 is the same as that of the matrix when the distance reaches 350 μm. The micro-hardness of the outer layer is not the highest because the outer layer near the sand mould unavoidably contains shrinkage porosity and the fusion is imperfect because the liquid metal was cooling at a high rate. Enough energy could be attained from the matrix at a small distance from the surface to allow the alloying element to mix with the matrix, forming a compact microstructure. Therefore, the mirco-hardness of the the subsurface layer is higher than that at the surface.

The aluminum element content of the alloying surface layer is dependent on the fraction of matrix and new phases. Due to the inadequacy of Al diffusion at the surface, Al element has a high weight fraction, which can reach 40%. The Sub-surface has a lower cooling rate, allowing a perfect diffusion of alloying element. The Al content declines gradually with distance from the surface. The micro-hardness curve shows a rather similar pattern to the aluminum content curve.

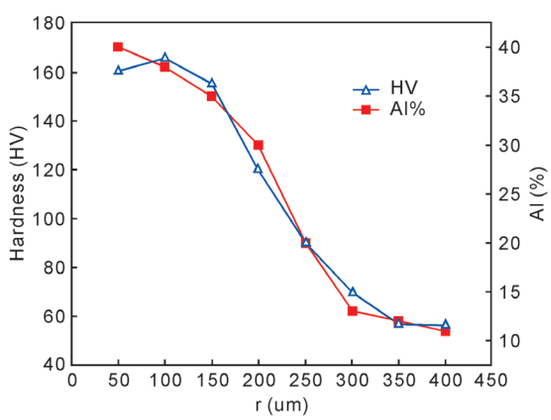

Fig.6: Distributions of HV Hardness and Al content along the direction of sample from the surface to the matrix

2.3.2 Corrosion properties

In order to examine the corrosion resistance of the alloying layer, the electrochemical property of the surface layer was evaluated in simulated sea water corrosion tests with 3.5wt%-NaCl solution at room temperature. Figure 7 shows polarization curves of samples under different conditions. Samples 1 to 3 are as-cast, with 0.3 mm and 0.5 mm coating, respectively. From the polarization curves, it shows that the Ecorr (V) of the as-cast sample is low compared to the surface alloying samples. The Ecorr (V) is increased and the Icorr (A) declined gradually with the increase of alloying coating thickness. So the corrosion resistance trend is: sample 3 >

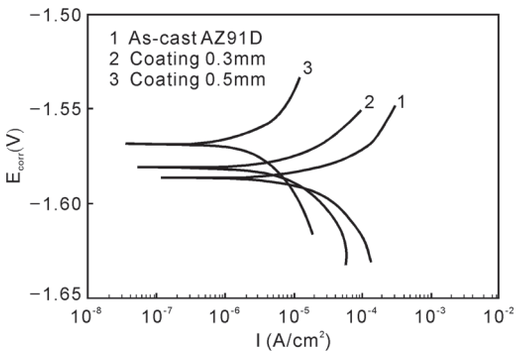

Fig. 7: Polarization curves of magnesium alloys under different conditions in 3.5% NaCl solution with a scanning rate of 0.2 mV/s

sample 2 > sample 1. Moreover, the corrosion rate calculated according to the electrochemical parameters listed in Table 3, shows that the corrosion resistance is improved by up to 5 times after surface alloying treatment compared to that of the as-cast samples.

In the initial stages of electrochemical corrosion test, bubbles are found attached on each work area surface. It is obvious that the bubbles on the as-cast samples are bigger and denser than those on the alloying samples. Those bubbles would get away from the surface when they are big enough. The number of bubbles shows an evident reduction when the coating thickness is 0.3 mm, and a significant further reduction when the coating thickness is 0.5 mm. The corrosion current density declines and corrosion resistance is enhanced as a result of the alloying layer.

In order to further study the effect of surface alloying on the corrosion resistance, immersion tests were carried out in 3.5wt% NaCl solution, with an immersion time of 24 hours. The macro-morphologies of the corrosion specimens are shown in Fig. 8. It can be seen that the alloying samples were severely corroded. The eroded pits are present where the corrosion products peel off. On the contrary, the as-cast AZ91D was relatively less and uniformly corroded. This would suggest that the alloying layer is not contributing to the corrosion resistance of alloy, but accelerating the corrosion. This may be caused by a lack of continuity of the alloying layer on the surface, not completely covering the whole surface. On one hand, β phase is propitious to protect the matrix. But on the other hand, it would increase the corrosion rate of the alloy if the β phase and α phase form a galvanic current on account of a non-continuous distribution. So the continuity of the β phase is very important. The barrier effect only dominates the corrosion process when the β precipitates are evenly distributed. Therefore, the quality of the alloying layer can be measured in terms of microstructure whether is continuous and uniform.

Table 3: Electrochemical parameters based on polarization curves in Fig. 7

Sample	AZ91D	Coating 0.3 mm	Coating 0.5 mm
Ecorr（V）	-1.5913	-1.5758	-1.5628
Icorr（A/cm^2）	1.90752 e^{-4}	5.44023 e^{-5}	2.91649 e^{-5}
Corrosion rate（mmPY）	10.0578	2.8685	1.5372

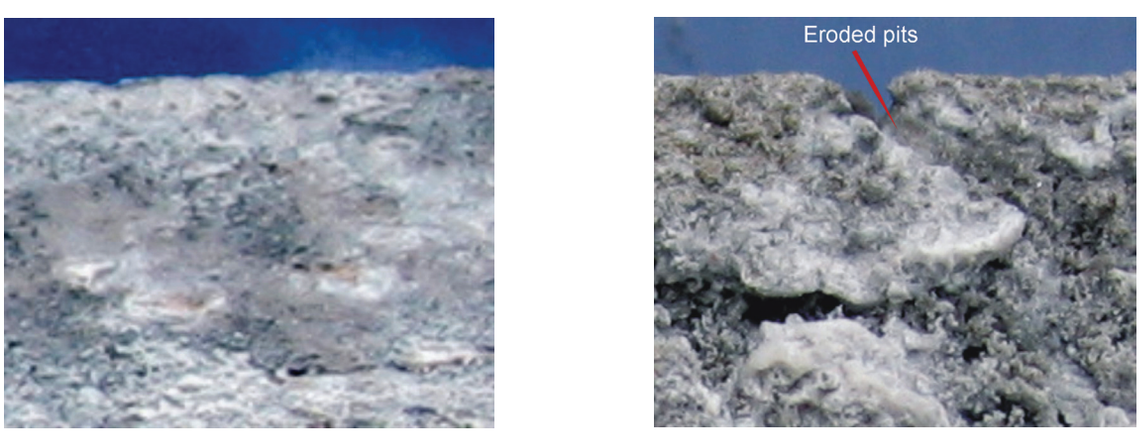

(a) As-cast AZ91D alloy (b) Surface alloying sample

Fig. 8: The corrosion morphologies of as-casting and alloying samples

3 Conclusions

(1) Aluminium powder was used as the alloying element and the alloying coating constitution was optimized. The Mg-alloy surface alloying layer has been successfully fabricated by EPC technology, but the continuity of the surface microstructure needs to be improved. As a new surface modification method, the EPC surface alloying layer formation mechanism and interface theories need to further study in the future, such as in the principle of thermodynamics and kinetics during the alloying process.

(2) The alloying coating thickness has a strong effect on

the surface microstructure of Mg-alloy under conditions of pouring temperature being 780℃ and negative pressure being 0.2 MPa. When the thickness of the alloying coating increases from 0.3 to 0.5 mm, the surface quality is enhanced in that the microstructure becomes denser and the thickness of alloying layer also increases.

(3) The micro-hardness at the surface layer of alloy is about HV150 and has a degressive trend from the surface to matrix. The highest micro-hardness reaches nearly HV170, about three times higher than that of the substrate. Electrochemical test suggests that the corrosion potential increases and the corrosion current density decreases for alloying samples compared to the as-cast samples. As a result, the corrosion resistance is increased by 5 times compared with as-cast samples.

References

[1] Aghion E, Bronfin B, Friedrich H, et al. The environmental impact of new magnesium alloys on the transportation industry. Magnesium Technology, TMS, 2004: 167–172.

[2] Myers P. Reducing transportation fuel consumption: how far should we go. In: Proceedings of the Society of Automotive Engineers, 1992, 10: 225–234.

[3] Makar G L and Kruger J. Corrosion of magnesium. International Materials Reviews,1993, 38(3) : 138 –153.

[4] Gray J E and Luan B. Protective coatings on magnesium and its alloys – A critical review. Journal of Alloys and Compounds, 2002, 336(1/2): 88–113.

[5] Jiang Y F, Zhai C Q, Liu L F, Zhu Y P and Ding W J. Zn-Ni alloy coatings pulse-plated on magnesium alloy. Surface and Coatings Technology, 2005, 191(2/3): 393–399.

[6] Chong K Z and Shih T S. Conversion coating treatment for magnesium alloys by a permanganate phosphate solution. Material Chemistry and Physics, 2003, 80: 191–200.

[7] Hawke D and Albright D L. A phosphate permanganate conversion coating for magnesium. Metal Finishing,1995 (10): 34–38.

[8] Zhang R F, Shan D Y, Han E H and Zeng Z L. Status and prospect of anodization on magnesium and its alloys. The Chinese Journal of Nonferrous Metals, 2006, 16(7): 1136–1148.

[9] Zozulin A J and Bartak D E. Anodized coatings for magnesium alloys. Metal Finishing, 1994. 32(3): 39–44.

[10] Frank H, Renate W and Jana S. Characteristics of PVD coating on AZ31 hp magnesium alloys. Surface and Coatings Technology, 2003, 162: 261–268.

[11] Hoche H, Scheerer H, Probst D, et al. Plasma anodization as an environmental harmless method for the corrosion protection of magnesium alloys. Surface and Coatings Technology, 2003,174: 1002–1007.

[12] Wang J, Ding Y, Xu W, and Wang L L. The surface phosphating treatment of AZ31 magnesium alloys. Surface Technology. 2006, 35(2): 55–56.

[13] Ignat S, Sallamand P, Grevey D and Lambertin M. Magnesium alloys laser (Nd:YAG) cladding and alloying with side injection of aluminium powder. Applied Surface Science, 2004, 225: 124–134.

[14] Yang G R, Song W M, Lu J J, et al. Microstructure of surface composite Al_2O_3/Ni on copper substrate produced by vacuum infiltration casting. Material Seience and Engineering, 2006, 418 (1–2): 223–228.

[15] Li Zulai, JiangYehua, Zhou Rong, et al. Dry three-body abrasive wear behavior of WC reinforced iron matrix surface composites produced by V-EPC infiltration casting process. Wear, 2007, 262: 649–654.

[16] Mortensen A, Kouzeli M, Weber L, San Marchi C. Corrigendum to: on the tensile behavior of infiltrated alumina particle reinforced aluminium composites. Acta Materialia, 2003, 51, (20): 6493–6496.

[17] Chen H, Kaya M and Smith R W. Near net-shape long fibre reinforced inter-metallic matrix composites produced by reactive infiltration process. Materials, 1992, 13(4-5): 180–183.

[18] Yang Guirong, Hao Yuan, Song Wenming, et al. Effect of some parameters of formation on surface graphite- bronze composite layer prepared by vacuum infiltration casting technique. In: The Eighth China-Russian International Conference on New Materials and Technologies, 2005: 510–517.

The study was financially supported by the National Natural Science Foundation of China (No. 50775085)